Journal of Earthquake Prediction Research **8** (2000) 351–360.

Theoretical Scaling Laws for Fault Length, Seismic Electromagnetic Signals (SEMS) and Maximum Appearance Area

Motoji Ikeya, Hiroshi Matsumoto, Qinghua Huang and Shynji Takaki

Department of Earth and Space Sciences, Graduate School of Science, Osaka University, 1–1 Machikaneyama, Toyonaka, Osaka 560–0043, Japan

Abstract. Scaling laws between the moment magnitude, M_W and a quantity, X have been theoretically derived. Forms of $\log X = bM_W + c$ and $M_W = b'\log X + c'$, where b, c, b' and c' are constants, are equivalent to a power law of the earthquake moment, $M_0 = kX^l$, using $M_W = (\log M_0 - 9.1)/1.5$ and $l = 1.5/b = 1.5b'$ and $k = 10^{(9.1-1.5c)/b} = 10^{9.1+1.5c'}$. The stress drop, $\Delta\sigma$ and fault length $2a$ give $M_0 = \Delta\sigma(2a)^3$ and $M_0 = \Delta\sigma h(2a)^2$ for small and large earthquakes, where h is the depth of the brittle–ductile seismogenic transition layer; $l = 3$ and 2 for $X = 2a$ lead to $b = 0.50$ and 0.75 ($b' = 2.0$ and 1.33). The intensity of seismic electromagnetic signals (SEMS), F, was calculated from an ensemble of dipolar charges leading to $\log FR = bM_W + c$, where R is the distance from the source and $b = 0.5$ and 0.375 for small and large earthquakes. The maximum area of appearance of unusual animal behavior, r_{max} was determined as $M_W = b'\log F_{min} r_{max} + c'$ ($b' = 2.00$ and 2.67) which agrees with the empirical equation by Rikitake, $M = 2.6\log r_{max} - 0.89$ for $F_{min} = 10^{-5}$ V / m.

1. Introduction

Empirical scaling laws of earthquakes have been used to estimate the relations between the earthquake magnitude, M and some physical quantity, X either in a form of $\log X = bM + c$ or $M = b'\log X + c'$ in seismology, where b, c, b' and c' are constants empirically determined (Dambara, 1981; Chen and Bai, 1992). Note that we use the same terms, b and b' as the b–value in the Gutenberg–Richter relation describing the earthquake frequency, n and its relation with the magnitude, $\log n = bM + c$. The latter has been discussed frequently from self–similarity effect of earthquakes (Bak and Tang, 1989; Ito and Matsuzaki, 1990). Departure from the relation at large earthquakes was ascribed to the finite thickness of the underground inelastic fault zone (Rikitake, 1975; Rundle, 1989, 1993).

The definition of earthquake magnitude M_W with the earthquake moment, M_0 (Kanamori and Anderson, 1975) gives a power law of the quantity X as $M_0 = kX^l$ for scaling laws, which gives us an insight on the background physics. Physical parameters such as the energy of earthquakes, fault length and so on were discussed considering the seismogenic layers of Earth (Rikitake, 1975, 1986, 1994; Pacheco et al., 1992). Theoretical b–values for small and large earthquakes were obtained for main shocks, aftershocks and foreshocks considering a finite thickness of 20 km for the seismogenic layer (Ikeya and Huang, 1997).

Seismic electromagnetic signal (SEMS) intensity, F known as the VAN method gave an empirical equation of $\log F = 0.37M + c$ (Varatos et al., 1996), which was explained as the intensity of electromagnetic (EM) waves at ultra low frequency (ULF) (Ikeya et al., 1997). Although the VAN method is still controversial, the scaling relations give an insight to the underlying physics of the VAN method. In this paper, physical meanings of the empirical scaling laws are discussed for small and large earthquakes in the layered structure of Earth. A scaling law of seismic electromagnetic signal (SEMS) has been derived considering an ensemble of dipolar charges, presumably arising from quartz grains. Charges are generated by stress changes and decay in conductive Earth as discussed in an EM model of a fault following a mathematical model of a fault.

2. Scaling Laws and Power Law for Fault Length and Area

2.1. Power Law of the Earthquake Moment

The relation between an earthquake–related physical quantity, X and the magnitude, M has empirically been discussed as scaling laws in two forms of

$$\log X = bM_{\mathrm{W}} + c \ , \tag{1}$$

$$M_{\mathrm{W}} = b' \log X + c \ , \tag{2}$$

where b, c, b' and c' are constants and the moment magnitude, M_{W} is related with the earthquake moment, M_0 (Kanamori, 1978) in SI unit as $M_{\mathrm{W}} = (\log M_0 - 9.1)/1.5$ in seismology. We assume $M = M_{\mathrm{W}}$ here and obtain a power law of $M_0 = kX^l$ as given in the Appendix 1. The power index l obtained from b and b' gives physical insight as tabulated in Table 1.

Table 1. Simple power laws of a physical quantity, X and the earthquake moment, M_0 for parameters b and b' in the scaling laws using the moment magnitude, M_{W} as given in equations, $\log X = bM_{\mathrm{W}} + c$ and $M_{\mathrm{W}} = b' \log X + c'$

Relation between X and M_0		b	b' $(1/b)$	Examples for X
$X \propto M_0^{1/6}$	$M_0 \propto X^6$	0.25	4.0	
$X \propto M_0^{1/4}$	$M_0 \propto X^4$	0.375	2.667	ΔV in the VAN method (Ikeya et al., 1997)
$X \propto M_0^{1/3}$	$M_0 \propto X^3$	0.50	2.0	fault length for $A = (2a)^2$
$X \propto M_0^{1/2}$	$M_0 \propto X^2$	0.75	1.33	fault length $A = 2ah$ for $M_0 = 2aA\Delta\sigma = \Delta\sigma(2a)^2 h$
$X \propto M_0^{2/3}$	$M_0 \propto X^{3/2}$	1.0	1.0	earthquake frequency
$X \propto M_0$	$M_0 \propto X$	1.50	0.667	earthquake energy

2.2. Small and Large Earthquakes $M_{\mathrm{W}} < 6.6$ and $M_{\mathrm{W}} > 6.6$

The earthquake moment, M_0, is defined as $M_0 = \mu DA$ in a mathematical model of a fault using the rigidity of the earth, μ, displacement of a fault, D and the area of a fault plane, A. Using the stress drop, $\Delta\sigma = \mu(D/2a)$ and fault length, $2a$,

$$M_0 = \mu DA = \Delta\sigma(2aA) \ . \tag{3}$$

A small ($2a < h$) and a large earthquake ($2a > h$) are considered, where h is the depth of the brittle–ductile transition layer under which the deformation is made smoothly without fractures (Rikitake, 1975; Pacheco et al., 1992; Scholz, 1994, 1987; Pegler and Das, 1996). The area of a fault plane, $A = (2a)^2$ and $A = 2ah$ and so $M_0 = (2a)^3 \Delta\sigma$ and $M_0 = (2a)^2 h \Delta\sigma$ for small and large earthquakes, respectively. The critical transition value of $M_{W_c} = 6.6$ is obtained for $h = 2a =$

2×10^4 m and $\Delta\sigma=1.25\times10^6$ N / m^2 (Romanowicz, 1992). Definition of M_W indicates $M_{W_c}=6.6\pm0.6$ for the factor 2 difference of h and $M_{W_c}=6.6\pm0.2$ for the factor 2 difference of $\Delta\sigma$.

2.3. *Fault Length 2a and Those Related with 2a*

(a) Fault length, $2a$:

A fault length is expressed as $2a=(M_0\Delta\sigma)^{1/3}$ and $2a=(M_0/h\Delta\sigma)^{1/2}$ *for small and large earthquakes. Hence, the scaling laws of 2a* is theoretically using $M_W=(\log M_0-9.1)/1.5$ as

$$M_W<6.6:\ \log 2a=0.5M_W+1.0\ , \tag{4}$$

$$M_W<6.6:\ \log 2a=0.75M_W-0.65\ , \tag{5}$$

and so

$$M_W<6.6:\ M_W=2.0\log 2a-2.0\ , \tag{6}$$

$$M_W<6.6:\ M_W=1.33\log 2a+0.87\ . \tag{7}$$

for $\Delta\sigma=1.25\times10^6$ N / m^2. Eq. (4) is in agreement with the relation derived from other model as $\log(2a)=0.5M_W+1.1$ (Chen and Bai, 1992). Some empirical relation, $\log 2a=0.6M-2.9$ for $2a$ in km was obtained without considering the seismogenic layers. This is equivalent to $\log 2a=0.6M_W+0.1$ and is very close to the average of mixing Eq. (4) and Eq. (5); the simple average is $\log 2a=0.625M_W+0.175$.

(b) A quantity, X proportional to $2a$:

$X=\gamma(2a)$ gives similar formula as

$$M_W<6.6:\ \log X=0.5M_W+1.0+\log\gamma\ , \tag{8}$$

$$M_W>6.6:\ \log X=0.75M_W-0.65+\log\gamma\ . \tag{9}$$

Fault displacement, D, stress drop is given as $\Delta\sigma=\mu(D/2a)$. Hence, $D=2a\Delta\sigma/\mu$ and so $\gamma=\Delta\sigma/\mu=1.25\times10^6$ N / m^2 / 3.3×10^{10} N / m$^2=3.75\times10^{-5}$. Thus, corresponding equations are

$$M_W<6.6:\ \log D=0.5M_W-3.45\ , \tag{10}$$

$$M_W>6.6:\ \log D=0.75M_W-4.10\ , \tag{11}$$

which correspond to empirical equation of $\log D=0.6M-4.0$ in Japan and $\log D=0.5M_W-3.34$ by Chen and Bai (1992). Note that the SI unit is used here, whereas most empirical values are in cgs unit or in the unit of km for the length.

2.4. *Radius of Deformation Area and Aftershock Area*

(a) Radius of deformation r:

Dambara (1981) obtained the empirical relation between the mean radius, r (km) of crustal deformation associated with earthquakes and the magnitude M, as $M=1.96\log r+4.43$ ($M=1.96\log r-1.45$ in SI unit). If $r=a$, the empirical relation of $M=1.96\log 2a-2.05$, which would roughly agree with the theoretical Eq. (6). This theory suggests us to reexamine the data in Fig.1 and forced us to fit into two theoretical lines of Eq. (6) and Eq. (7).

(b) Area of a fault plane A:

The area are $A=(2a)^2$ and $A=2ah$ for large and small earthquakes. Hence,

$$M_W < 6.6:\ M_W = \log A - 2.0\ , \tag{12}$$

$$M_W > 6.6:\ M_W = 1.33\log A - 4.85\ . \tag{13}$$

Rikitake (1975) dealt with the empirical aftershock area as $M = \log A_a - 2.3$ in SI unit, which agrees fairly well with Equation (12).

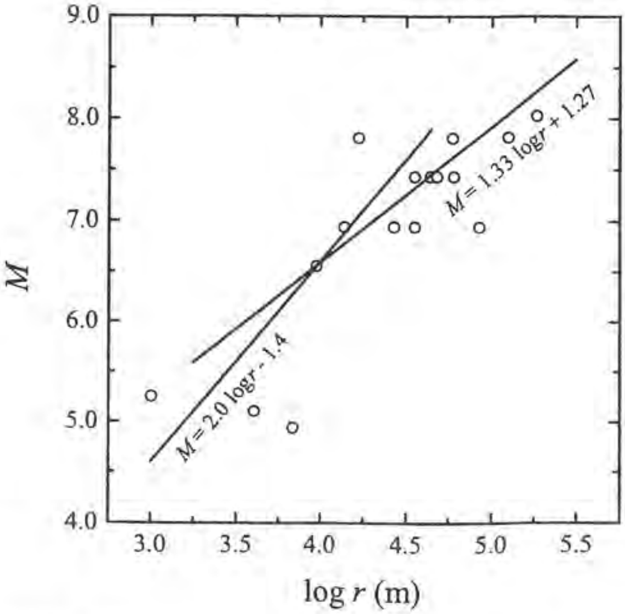

Fig. 1. An empirical relation between the magnitude and mean radius, r of crustal deformation associated with earthquakes. Circles represent observations. Two branches of $M = 2.0\log r - 1.4$ and $M = 1.33\log r + 1.27$ with a break at $M = 6.6$ are theoretically derived for the case of $r = a$, where a is half length of a fault. Empirically, $M = 1.96\log r - 1.45$ by Dambara (1981).

3. Intensity of Earthquake Precursors

3.1. Seismic Electric Signal (SES): Empirical Relation of SEMS

Piezoelectricity used to explain earthquake lightning was once discarded because free charges in conductive Earth compensate the piezoelectric polarization in a short time (Finkelstein and Powell, 1970). It is, however, these free charges that are released by the stress changes before the major shock (Ikeya and Takaki, 1996). The free charges on both edge of a quartz grain with a cube length a' have a dipolar moment p_i. An ensemble of electric dipoles, p_i, having a total dipole moment $P = \Sigma p_i$ in a fault zone will generate intense EM waves with the Poynting vector S (Ikeya et al., 1997a) and be observed by an observer at the distance R as given in Fig. 2.

Free charges were generated as the stress changes at the surface of a quartz grain as

$$\mathrm{d}q / \mathrm{d}t = -\alpha(\mathrm{d}\sigma / \mathrm{d}t) - q / \varepsilon\rho\ , \tag{14}$$

where α is the charge generation constant, ε, the dielectric constant, and ρ, resistivity of quartz bearing rocks. In our tentative model, α is a piezoelectric constant ($\alpha = 2 \times 10^{-12}$ C / N for quartz) for a mechanism of piezo–compensating free charges. It may be electrokinetic potential. The second term is due to the decay through conductive Earth. The free charges, $+q$ and $-q$ recombine with a time constant, $\varepsilon\rho = 70$–0.7 μs for $\varepsilon^* = \varepsilon / \varepsilon_0 = 8$ and $\rho = 10^6$–10^4 Ωm for granite; the decay through the quartz grain with a high resistivity of $\rho_{\text{quartz}} = 10^{15}$ Ωm is almost negligible since the charges move through conductive feldspar.

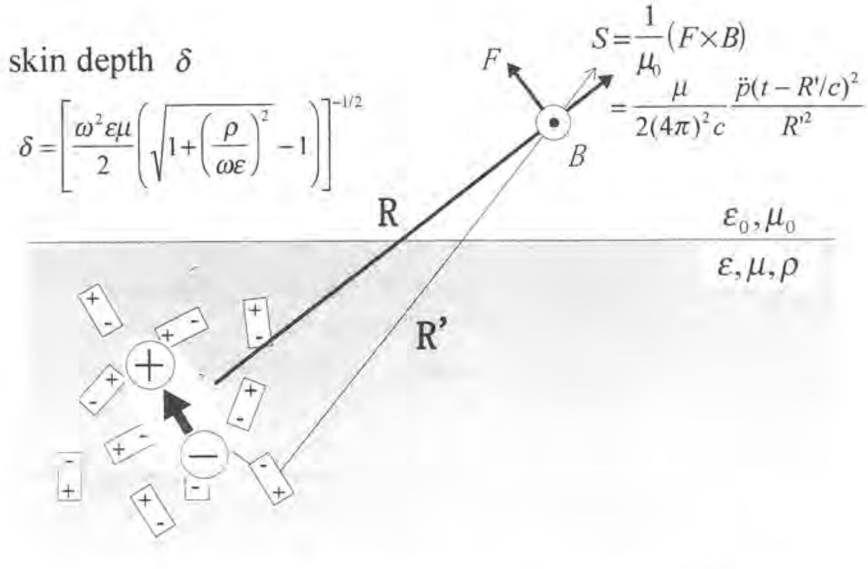

Fig. 2. A schematic drawing of the generation mechanism of electromagnetic (EM) pulses from an ensemble of dipolar charges, p_i and of observation at the distance R. Preseismic fractures and local stress changes are assumed for preseismic EM pulses and phenomena caused by them.

If the stress is released exponentially, $\sigma(t) = \sigma_1 + \Delta\sigma \exp(-t / \tau)$, where σ_1 and $\Delta\sigma$ are remnant stress and stress drop, respectively, Eq. (14) under the condition of $q = 0$ at $t = 0$ gives a pulsed charge $\pm q$ separated for the distance of $2a'$ as

$$q(t) = \alpha\Delta\sigma\, [\varepsilon\rho / (\tau - \varepsilon\rho)]\, (e^{-t/\tau} - e^{-t/\varepsilon\rho}) \; . \tag{15}$$

The pulse shape with the risetime of $\varepsilon\rho$ and the decay time of τ for $\tau > \varepsilon\rho$ (or vise versa for $\tau < \varepsilon\rho$). Hence, the dipole moment is $p_i(t) = q(t)(2a')^3$.

The Poynting vector, S_i, from a dipole p_i is reciprocally proportional to the square of the distance, R_i, from the hypocenter as given by

$$S_i(R_i, t) = (1 / 4\pi R_i)^2 (\mu_0 / c)\, [d^2 p_i / dt^2]^2 \sin^2\theta_i \; , \tag{16}$$

where c is the speed of light and θ_i is the angle between the vector p_i and the distance vector R_i ($R_i = R - r_i$). The average radiation energy for a dipole is obtained by integrating for all direction, i.e., $\sin^2\theta_i = 2 / 3$. The radiation energy for a dipole is obtained by integrating for all direction

$$W_i = (1/4\pi\varepsilon)(2/3c^3)[\mathrm{d}^2 p_i/\mathrm{d}t^2]^2 \ . \tag{17}$$

Using $p_i(t)=q(t)(2a')^3$ and so

$$\mathrm{d}^2 p_i/\mathrm{d}t^2 = \alpha\Delta\sigma(2a')^3\,[\varepsilon\rho/(\tau-\varepsilon\rho)][\mathrm{e}^{-t/\tau}/\tau^2 - \mathrm{e}^{-t/\varepsilon\rho}/\varepsilon^2\rho^2] \tag{18}$$

$$W_i = (1/4\pi\varepsilon)[2/(3c^3)]\{\alpha\Delta\sigma(2a')^3\,[\varepsilon\rho/(\tau-\varepsilon\rho)][\mathrm{e}^{-t/\tau}/\tau^2 - \mathrm{e}^{-t/\varepsilon\rho}/\varepsilon^2\rho^2]\} \ . \tag{19}$$

The energy for a single dipole is by integrating for the time from zero to infinite,

$$W_i = (1/4\pi\varepsilon)[2/(3c^3)]\{\alpha(2a')^3\Delta\sigma^2\,[\varepsilon\rho/(\tau-\varepsilon\rho)]\}^2\,[1/2\tau^3 - 2/(\tau+\varepsilon\rho)\tau\varepsilon\rho + 1/2\varepsilon^3\rho^3] \ . \tag{20}$$

The total number of quartz grains n at the fault zone with length $2a$ and the area A is given using the volume fraction of quartz in granitic rocks, η as $n=2aA\eta/(2a')$ * T3 . The earthquake moment in a mathematical model of a fault is given as $M_0=2aA\Delta\sigma$. Hence, n is given as

$$n = 2aA\eta/(2a')^3 = (\eta M_0/\Delta\sigma)/(2a')^3 \ . \tag{21}$$

Considering the quartz grain as a small fault with a length a', a virtual earthquake moment of $M'_0=(2a')$ * T3 $\Delta\sigma$ is introduced. Then, the total radiation energy at the distance R $(R \gg r_i)$ is

$$E = \Sigma W_i/4\pi R^2 = nW_i/4\pi R^2 = (1/4\pi R^2)(1/4\pi\varepsilon)[1/(3c^3)](\eta\alpha M_0\alpha M'_0)(\tau^2+3\tau\varepsilon\rho + \varepsilon^2\rho^2)/[\varepsilon\rho\tau^3(\tau+\varepsilon\rho)] \ . \tag{22}$$

The pulse width of radiation is of the order of τ or $\varepsilon\rho$ and so much smaller than the fault displacement time τ_f in the mathematical model of a fault. Suppose that the number of quasidipoles which radiate the EM waves decrease exponentially i.e., $N(t)=(n/\tau_f)\exp(-t/\tau_f)$, the energy of EM waves are given as $E(t)=(E/\tau_f)\exp(-t/\tau_f)$. Although the high frequency component is lost by introducing τ_f and large deviation statistics may be needed in reality, the initial energy density is E/τ_f. The initial electric field intensity, F is given using $F=(\mu cS)^{1/2}=19.8(E/\tau_f)^{1/2}$ as

$$F = (1/4\pi R)\{(1/\varepsilon)(1/3c^3)(\eta\alpha M_0/\tau_f)(\alpha M'_0)(\tau^2-3\tau\varepsilon\rho+\varepsilon^2\rho^2)/[\varepsilon\rho\tau^3(\tau+\varepsilon\rho)]\}^{1/2} \ . \tag{23}$$

The displacement time is given as $\tau_f=2(\alpha/\beta)(\Delta\sigma/\sigma_0)$ in a mathematical model of a fault using the rate of stress drop, $\Delta\sigma/\sigma_0$ and the velocity of S-waves, β. For earthquakes $M_W<6.6$ and $M_W>6.6$, $M_0=2aA\Delta\sigma=(2a)^3\Delta\sigma$ and $M_0=2aA\Delta\sigma=h(2a)^2\Delta\sigma$, where h is the depth of the brittle-ductile seismogenic transition layer. Hence, $\tau_f=(M_0/\Delta\sigma)^{1/3}(\Delta\sigma/\sigma_0)/\beta$ and $\tau_f=(M_0/h\Delta\sigma)^{1/2}(\Delta\sigma/\sigma_0)/\beta$ give a proportionality of $FR \propto M_0^{1/3}$ and $FR \propto M_0^{1/4}$ respectively. The scaling laws are

$$M_W < 6.6: \qquad \log FR = 0.500 M_W + c_1 \ . \tag{24}$$

$$M_W > 6.6: \qquad \log FR = 0.375 M_W + c_2 \ . \tag{25}$$

The latter happens to coincide with an early empirical relation of $\log FR=0.37M+c$ in the VAN method (Varatos and Alexopoulos, 1984), though present calculation is for SEMS with the wavelength less than the distance R. If the signal intensity of the VAN method were the electric field of ULF (0.1 Hz or so), present treatment is not applicable. Furthermore, the decay during the propagation of the distance R in the conductive earth must be considered as $F\exp(-k'R)$, where k' is the imaginary part of the wavevector related with the skin depth $\delta=1/k'=(2\omega\mu/r)^{-1/2}$ for low frequency and $\delta = 2c\varepsilon\rho$ at high frequency range using the resistivity of Earth, ρ. This part will actually go into the constants c_1 and c_2. This factor is negligible for a low frequency; $\delta = 16$ km at 10 Hz for bedrock granite of $\rho = 10^4$ Ωm. Theoretical calculation of logFR was made using piezoelectric constant as a charge generation constant as shown in Fig. 3 for different ρ of bedrock granite $\varepsilon^* = 8$.

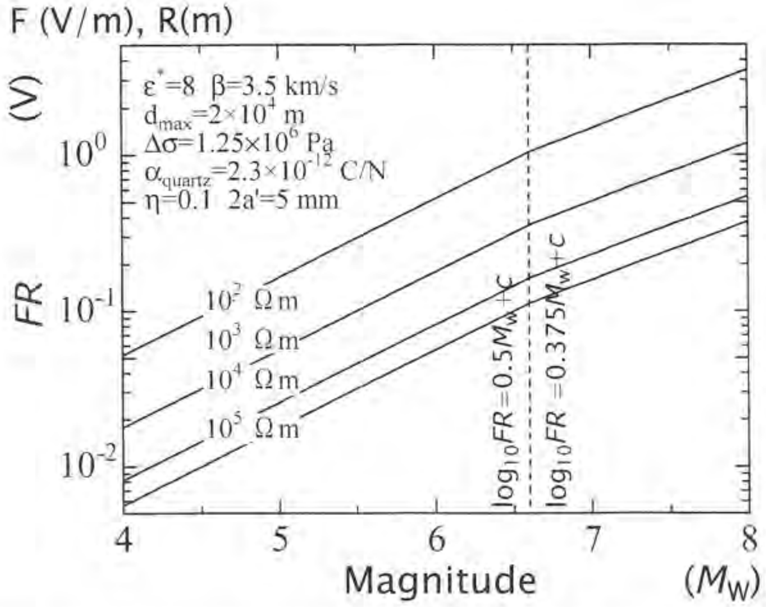

Fig. 3. A theoretical calculation of logFR for seismic electric signals as a function of the moment magnitude, M_W by averaging the pulses in an interval of the fault displacement time, τ_f. The large deviation, which might give unusual animal behavior, is averaged out in this theory. One can still estimate $FR = 0.5$ for $\rho = 10^3$ Ωm leading to $F = 5$ μV / m for $R = 10^4$ m in agreement with the results by the VAN method, and 1.3×10^{-8} V / m at the satellite position of $R = 3.6 \times 10^7$ m (36,000 km).

3.2. Area of Seismic Unusual Animal Behavior

Present theory of SEMS has further been extended to the maximum appearance radius of unusual animal behavior before earthquakes considering the hypothesis that animal responded to preseismic SEMS. Scientists are skeptical of retrospectively reported stories of unusual animal behavior. This section is therefore based on speculation based on the observation of lay citizen rather than on data observed by scientists. However, the manipulation of the scaling relation given here under the hypothesis of electric field stimuli gives the minimum electric field from the reported maximum area of observation in Japan and China (Rikitake, 1994).

An empirical equation of the maximum radius, r_{max} in km given in Fig. 4 is

$$M = 2.67\log r_{max} - 0.87 \ . \quad (26)$$

We simply assume here that the unusual behavior is an electro-physiological response to seismic electric stimuli or field-avoidance behavior as discussed previously (Ikeya et al., 1996a, b). Then, the observed area would be at a place where the electric field intensity of EM waves is larger than a critical one, F_c of the order of 10 V / m for ordinary animals and 0.5–5 V / m for sensitive one like catfish (Ikeya et al., 1998). The maximum radius of observation, r_{max} is obtained for a condition of $F > F_{min}$ using Eq. (24) and Eq. (25) for $FR = F_{min} r_{max}$, which leads to

$$M_W < 6.6: \qquad M_W = 2.000 \log r_{max} + c_1 \ , \tag{27}$$

$$M_W > 6.6: \qquad M_W = 2.667 \log r_{max} + c_2 \ , \tag{28}$$

where the constants $c_1 = 0.58$ and $c_2 = -0.91$ if adjusted to agree with the empirical equation (26) at $M_W = 6.6$ and $\log r_{max} = 2.8$. Theoretical lines fitted to the empirical data by Rikitake (1986) are shown in Fig. 4.

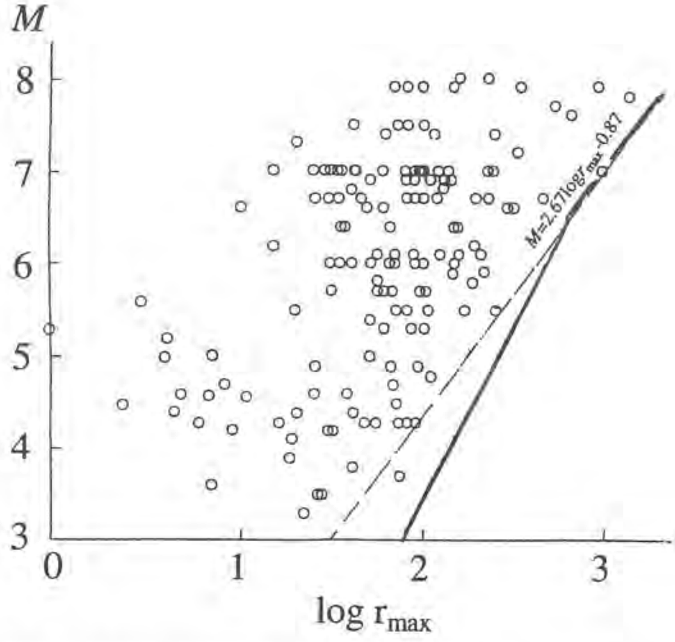

Fig. 4. An empirical scaling relation between the magnitude and the maximum distance of unusual animal behavior by Rikitake and theoretical lines under the assumption that animals are excited by electromagnetic pulses larger than a critical electric field intensity, F_c.

Empirical equations of $\log F_{min} r_{max} = 0.375 M_W - 0.8$ and $M_W = 2.67 \log r_{max} - 0.87$ ($M_W = 2.67 \log r_{max} - 8.97$ in SI unit) (Rikitake, 1994) give a field intensity $\log F_{min} = -1.13$ or $F_{min} = 0.08$ V / km $= 8 \times 10^{-5}$ V / m well above the detection of aquatic animals with electrosensory organs such as shark and catfish ($F_{min} = 10^{-6}$ V / m) (Bastian, 1994), but less than those of ordinary animals (Ikeya, 1997). The data for SEMS is only for ULF or DC field for the VAN method and for a narrow frequency band for SEMS. Unusual animal behavior may be caused by peak height of pulsed electric field of around 0.1 ~ 10 μs as discussed in the previous works (Ikeya, 1996a, b).

4. Summary

The relations between a physical quantity, X and an earthquake moment magnitude, M_W in a form of $\log X = bM_W + c$ and $M_W = b'\log X + c'$ were deduced theoretically for fault length, area, SEMS and the maximum area of unusual animal behavior using a power law of the earthquake moment, M_0 to X.

Small and large earthquakes were considered $M_0 = kX^l$ for a fault plane with area A of $(2a)^2$ and $2ah$ for small and large earthquakes, where h is the depth of the brittle–ductile transition layer. The scaling relation of the intensity of seismic electromagnetic signals (SEMS) was derived theoretically and compared with empirical ones. Speculative discussion was added on the maximum appearance area of unusual animal behavior and the electric field intensity of SEMS.

Acknowledgments

We thank Mr. A. Tani for their discussion. This work is partially supported by the Grant in Aids from the Foundation of Osaka University and from the Kansai Research Foundation for technology promotion (KRF).

Appendix I.

Earthquake–related physical quantity, X is expressed by scaling laws in forms of $\log X = bM_W + c$ and $M_W = b'\log X + c'$ using the moment magnitude, M_W, where b, c, b' and c' are constants. These are equivalent to power laws of

$$M_0 = 10^{9.1 - 1.5c/b} X^{1.5/b} = 10^{9.1 + 1.5c'} X^{1.5b'} , \tag{3}$$

$$X = 10^{c - 6.07b} M_0^{b/1.5} = 10^{-(c' + 6.07)/b'} M_0^{1/1.5b'} , \tag{4}$$

which give $l = 1.5 / b = 1.5b'$ and $k = 10^{9.1 - 1.5c/b} = 10^{9.1 + 1.5c'}$. Typical scaling laws are summarized in Table 1.

References

Bak, P. and Tang, C., 1989. Earthquake as self organized critical phenomenon, J. Geophys. Res., Vol. 94, pp. 15635–15637.

Bastian, J. 1994. Electrosensory organs of aquatic animals, Physics Today, Vol. 47, pp. 30–37.

Chen, P. and Bai, T., 1992. Quantification relations between the source parameters, Acta Seismol. Sin., Vol. 5, pp. 435–446.

Dambara, T., 1981. Geodesy and earthquake prediction. In: Rikitake, T. (Ed.), Current research in earthquake prediction, Center for Academic Publication Japan, Japan Scientific Societies Press, Tokyo, pp. 167–220.

Finkelstein, D. and Poiwell, J., 1970. Earthquake lightning, Nature, Vol. 228, pp. 759–760.

Fukao, Y. and Furumoto, M., 1985. Hierarchy in earthquake size distribution, Phys. Earth Planet. Inter., Vol. 37, pp. 149–168.

Ikeya, M. and Takaki, S., 1996. Electromagnetic model of a fault for earthquake lightning, Jpn. J. Appl. Phys., Vol. 35, L355–357.

Ikeya, M., Takaki, S. and Takashimizu, D. 1996a. Electric shocks for seismic animal anomalous behaviors (SAABs), J. Phys. Soc. Japan, Vol. 65, pp. 710–712.

Ikeya, M., Huruta, H. Anzai, H. and Kajiwara, N., 1996b. Electric field effects on rats and sparrows for seismic animal anomalies (SAABs), Jpn J. Appl. Phys, Vol. 65, pp. 4587–4594.

Ikeya, M., Takaki, S., Matsumoto, H., Tani, A. and Komatsu, T., 1997a. Pulsed charge model of a fault behavior producing seismic electric signals, J. Circuit, Systems and Computers, Vol. 7, pp. 153–164.

Ikeya, M., Kinoshita, Y., Matsumoto, H., Takaki, S. and Yamanaka, C., 1997b. A model experiment of EM wave propagation over long distances using waveguide terminology, Jpn. J. Appl. Phys., Vol. 37, L1558–L1561.

Ikeya, M. and Huang Q. 1997. Earthquake frequency and moment magnitude relations for mainshock, aftershocks and foreshocks: Theoretical b–values, Episodes, Vol. 20, pp. 181–184.

Ikeya M., Matsuda, T. and Yamanaka, C., 1998. Reproduction of mimosa and clock anomalies before earthquakes: Are they "Alice in Wonderland Syndrome?" Proc. Japan Acad., 74, Ser. B, pp. 60–64.

Ito, K. and Matsuzaki, M., 1990. Earthquakes as self–organized critical phenomena, J. Geophys. Res., Vol. 95, pp. 6853–6860.

Kanamori, H. 1978. Quantification of earthquakes, Nature, Vol. 271, pp. 411–414.

Kanamori, H. and Anderson, 1975. Theoretical basis of some empirical relations in seismology, Bull. Seismol. Soc. Am., Vol. 65, pp. 1073–1095.

Matsuura, M. and Sato, T., 1997. Loading mechanism and scaling relation of large earthquakes, Tectonophys., Vol. 227, pp. 189–198.

Mogi, K. 1962. Magnitude–frequency relation for elastic shocks accompanying fractures of various materials and some related problems in earthquakes, Bull. Earthq. Res. Inst., Tokyo Univ., Vol. 40, pp. 831–853.

Pacheco, J.F., Scholz, C.H. and L.R. Sykes, 1992. Change in the frequency and size relationship from small to large earthquakes, Nature, Vol. 355, pp. 71–73.

Pegler, G. and Das, S. 1996. Analysis of the relationship between seismic moment and fault length for large crustal strike–slip earthquakes between 1977–1992, Geophys. Res. Lett., Vol. 23, pp. 905–908.

Rikitake, T., 1975. Dilatancy model and empirical formula for an earthquake area, Paleoph. Vol. 113, pp. 141–147.

Rikitake, T., 1986. Earthquake Precursor Phenomena — Database for Prediction, Univ. Tokyo Press, Tokyo (in Japanese).

Rikitake, T., 1994. Nature of macro–anomaly precursory to an earthquake, J. Phys. Earth, Vol. 42, pp. 149–163.

Romanowicz, B., 1992. Strike–slip earthquakes on quasi–vertical transcurrent faults: interferences for general scaling relations, Geophys. Res. Lett., Vol. 19, pp. 481–484.

Romanowicz, B. and Rundle, J.B., 1993. On scaling relations for large earthquakes, Bull. Seismol. Soc. Am., Vol. 83, pp. 1294–1297.

Rundle, J.B., 1989. Derivation of the complete Gutenberg–Richter magnitude–frequency relation using the principle of scale invariance, J. Geophys. Res., Vol. 94, pp. 12337–12342.

Rundle, J.B., 1993. Magnitude–frequency relation for earthquakes using a statistical mechanical approach, J. Geophys. Res., Vol. 98, pp. 21943–21949.

Scholz, C.H., 1987. Size distributions for large and small earthquakes, Bull. Seismol. Soc. Am., Vol. 87, pp. 1074–1077.

Scholz, C.H., 1994. A reappraisal of large earthquake scaling, Bull. Seismol. Soc. Am., Vol. 84, pp. 215–218.

Varatos, P. and Alexopoulos, K., 1984. Physical properties of the variations of the electric field of the Earth preceding earthquakes, Tectonophysics, Vol. 110, pp. 73–98.

Varatos, P., Lazanidou, M., Eftaxias, K., Antonopoulos, G., Marras, J. and Koparas, J., 1996. Short term earthquake prediction in Greece by seismic electric signals. In: Lighthill, S.J. ed., A critical review of VAN: earthquake prediction from seismic electric signals. WorldScientific, Singapore, pp. 29–76.